Optimization of a self antigen for presentation of multiple epitopes in cancer immunity

José A. Guevara-Patiño,[1] Manuel E. Engelhorn,[1] Mary Jo Turk,[1] Cailian Liu,[1] Fei Duan,[1,2] Gabrielle Rizzuto,[1,2] Adam D. Cohen,[1,2] Taha Merghoub,[1] Jedd D. Wolchok,[1,2] and Alan N. Houghton[1,2]

[1]Swim Across America Laboratory of Tumor Immunology, Memorial Sloan-Kettering Cancer Center, New York, New York, USA.
[2]Weill Medical and Graduate Schools of Cornell University, New York, New York, USA.

T cells recognizing self antigens expressed by cancer cells are prevalent in the immune repertoire. However, activation of these autoreactive T cells is limited by weak signals that are incapable of fully priming naive T cells, creating a state of tolerance or ignorance. Even if T cell activation occurs, immunity can be further restricted by a dominant response directed at only a single epitope. Enhanced antigen presentation of multiple epitopes was investigated as a strategy to overcome these barriers. Specific point mutations that create altered peptide ligands were introduced into the gene encoding a nonimmunogenic tissue self antigen expressed by melanoma, tyrosinase-related protein-1 (Tyrp1). Deficient asparagine-linked glycosylation, which was caused by additional mutations, produced altered protein trafficking and fate that increased antigen processing. Immunization of mice with mutated Tyrp1 DNA elicited cross-reactive CD8$^+$ T cell responses against multiple nonmutated epitopes of syngeneic Tyrp1 and against melanoma cells. These multispecific anti-Tyrp1 CD8$^+$ T cell responses led to rejection of poorly immunogenic melanoma and prolonged survival when immunization was started after tumor challenge. These studies demonstrate how rationally designed DNA vaccines directed against self antigens for enhanced antigen processing and presentation reveal novel self epitopes and elicit multispecific T cell responses to nonimmunogenic, nonmutated self antigens, enhancing immunity against cancer self antigens.

Introduction

T cells play a central role in immunity against cancer. Cancer antigens recognized by T cells are encoded by 2 broad categories of genes: those expressed by normal somatic and germ cells and those expressed only by cancer cells (e.g., due to mutations acquired during or after malignant transformation) (1, 2).

A question had been whether T cells capable of recognizing self antigens on cancer cells are present in the repertoire. Evidence shows that T cells are positively selected for survival during development in the thymus by signals elicited by self peptides complexed with MHC molecules (pMHCs) and maintained in the periphery by self pMHCs (3–7). Thus the repertoire of T cells develops and is maintained through self reactivity. To avoid autoimmunity, T cells with high avidity for self pMHCs are deleted, but more weakly self-reactive T cells survive.

This pool of T cells discriminates nonself antigens of pathogens by cross-reactivity to foreign peptides in the context of proinflammatory and costimulatory signals elicited by pathogens through activation of APCs. On the other hand, cognate self peptides are too weak to activate T cells, particularly in the absence of sufficient costimulation (8). A corollary to these observations is that, despite abundant self-reactive T cells in the peripheral immune system, initiation of T cell responses against self antigens on cancer are restricted by insufficient signals.

One strategy to overcome these limitations uses active immunization with orthologous gene products. Immunization with orthologs can overcome tolerance or ignorance to self antigens, including those expressed by cancer (9–17). This approach relies on small differences in amino acid sequences between orthologous proteins from mutations accumulated over tens of millions of years of evolution. One mechanism underlying increased immunogenicity of orthologous antigens relates to the augmented avidity of orthologous peptide for host MHC molecules relative to weak avidity of the cognate self peptide (13, 18, 19). Altered peptide ligands with increased avidity for MHC molecules can enhance interactions between pMHCs and T cell receptors to produce T cell activation (20).

The tyrosinase family represents prototypic tissue self antigens expressed by cancer. Tyrosinase-related protein-1 (Tyrp1) is the most abundant glycoprotein in melanocytes and pigmented melanomas and is recognized by autoantibodies in melanoma patients (21, 22). Mice are tolerant to Tyrp1, but tolerance is broken by orthologous antigen or syngeneic antigen expressed by vaccinia that results in weak tumor immunity (12, 14, 23). Notably, immunity against Tyrp1 is independent of CD8$^+$ T cells and is instead mediated by CD4-dependent, Th2-type autoantibodies (12, 14, 24).

To avoid relying on mutations selected through the millennial time frame of evolution, in the present study rationally selected mutations were introduced into the Tyrp1 gene to enhance antigen processing and presentation of multiple epitopes in order to determine whether it was possible to generate multivalent CD8$^+$ T cell responses. We were able to convert the inert syngeneic Tyrp1 cDNA to forms that induced multi-epitope, CD8$^+$-dependent, Th1-type melanoma immunity in mice. Such rationally designed, multivalent immunogens could be useful to direct specificity of responses in the context of nonspecific immune modulation therapies (25).

Nonstandard abbreviations used: Endo H, endoglycosidase H; exo-, fusion with exotoxin A domain; pMHC, peptide complexed with MHC molecules; Tyrp1, tyrosinase-related protein-1; Tyrp1ee, epitope-enriched Tyrp1; Tyrp1ee/ng, epitope-enriched, glycosylation-deficient Tyrp1; Tyrp1ng, glycosylation-deficient Tyrp1.

Conflict of interest: The authors have declared that no conflict of interest exists.

Citation for this article: *J. Clin. Invest.* **116**:1382–1390 (2006). doi:10.1172/JCI25591.

Table 1
Tyrp1 peptide optimization for MHC class I binding

Tyrp1 peptides	Wild-type Sequence	Optimized Mutation	Optimized Sequence
H2-K^b–restricted			
7	LPLAYISL	L9Y	LPYAYISL
175	NTPQFENI	I182L	NTPQFENL
222	TWHRYHLL	H224Y	TWYRYHLL
344	TPPFYSNS	S351L	TPPFYSNL
396	NDPIFVLL	P398Y	NDYIFVLL
522	YAEDYEEL	E524Y	YAYDYEEL
H2-D^b–restricted			
105	FSGHNCGTC	C113M	FSGHNCGTM
252	ATGKNVCDV	V260M	ATGKNVCDM
455	TAPDNLGYA	A463M	TAPDNLGYM
481	IAVVAALLL	A485N	IAVVNALLL
HLA-A*0201–restricted			
188	FVWTHYYSV	V189L	FLWTHYYSV
213	FSHEGPAFL	S214I	FIHEGPAFL
238	MLQEPSFSL	M238Y	YLQEPSFSL
249	WNFATGKNV	N250L	WLFATGKNV
401	VLLHTFTDA	A409V	VLLHTFTDV
439	NMVPFWPPV	N439Y	YMVPFWPPV

Results

Tyrp1 DNA constructs. Immunization against multiple epitopes is associated with improved immunity in infectious disease models (26, 27). We decided to investigate active immunization against multiple MHC class I epitopes using the melanocyte-specific self antigen mouse Tyrp1. This autoantigen has only been connected to antibody-dependent, CD8-independent immunity, and to our knowledge no MHC class I–restricted epitopes have been previously identified in Tyrp1 (12, 14, 24). The strategy was to induce a potentially broad CD8$^+$ T cell response against Tyrp1. To do this, we introduced a series of mutations in mouse Tyrp1, creating multiple altered peptide ligands for increased MHC presentation. Antigen processing and presentation were further enhanced by creating deficient glycosylation sites. The panel of Tyrp1 DNA plasmid constructs included nonmutated syngeneic (wild-type) mouse Tyrp1 (Tyrp1); epitope-enriched Tyrp1 (Tyrp1ee), incorporating 10 point mutations to create potential altered peptide ligands (Table 1); Tyrp1 mutated at 6 positions to generate deficient Asn-linked glycosylation sites (Tyrp1ng), but not optimized for MHC class I binding; and combined epitope-enriched, glycosylation-deficient Tyrp1 (Tyrp1ee/ng). Construction and characterization of these vectors is described in the following paragraphs.

Epitope-enriched Tyrp1. The Tyrp1ee DNA constructs incorporated multiple amino acid mutations that were predicted to increase epitope binding to MHC class I molecules H2-K^b and H2-D^b. To design this construct, we identified 10 self peptides in Tyrp1 with predicted low-level binding to MHC class I molecules using existing matrices (28). T cells recognizing low-affinity, tissue-specific self peptides are expected to escape thymic deletion. Mutated peptides with single amino acid changes at candidate MHC anchor sites that were predicted to create altered peptide ligands with enhanced MHC class I binding were compared with nonmutated wild-type peptides. Eight of 10 mutated peptides had enhanced MHC class I binding compared with their wild-type counterparts by MHC class I stabilization assays (Figure 1), using the transporter associated with antigen processing 2–deficient (TAP2–deficient) RMA-S cell line (29, 30). The Tyrp1ee cDNA variant was constructed by introducing single nucleotide mutations by site-directed mutagenesis into full-length mouse Tyrp1 cDNA (22, 31) (Table 1, H2-D^b– and H2-K^b–optimized peptides).

Tyrp1 with deficient Asn-linked glycosylation. Tyrp1 is a transmembrane protein that, in its mature state, contains complex Asn-linked sialylated sugars. Tyrp1 carbohydrates are processed from high mannose to intermediate and complex glycans during movement from the ER through the Golgi complex (32–34). Tyrp1 contains 6 potential Asn-linked glycosylation sites in the lumenal domain (33–35). Our prior studies have shown that these glycans differentially determine egress from the ER, movement through the Golgi to the endosomal pathway, stability in the endosomal pathway, and overall stability of Tyrp1 (34).

Six mutations (Asn→Gln) were introduced into the potential glycosylation sites of Tyrp1 and Tyrp1ee to produce deficient Asn-linked sites Tyrp1ng and Tyrp1ee/ng (see Methods), the latter protein incorporating both sets of mutations. We predicted that these mutations would promote ER retention, enhanced susceptibility to proteolytic digestion, and decreased stability, thereby increasing MHC class I antigen processing, perhaps guided by an ER misfolded protein response (34, 36–38).

Biosynthesis of epitope-enriched and glycosylation-deficient Tyrp1 mutants. To assess the stability of Tyrp1ee and Tyrp1ee/ng proteins compared with wild-type Tyrp1, Cos-7 cells were transiently transfected with DNA encoding each of the Tyrp1 constructs containing a Flag tag at the carboxyl terminus. New protein synthesis was blocked with muconomycin A at 24 hours. At this time point (designated 0), wild-type Tyrp1 and Tyrp1ee were detected as single bands of approximately 75 kDa (Figure 2A). Interestingly, Tyrp1ee/ng was consistently observed as a ladder of bands ranging from approximately 75 kDa to approximately 59–60 kDa, always with a weak top 75-kDa band

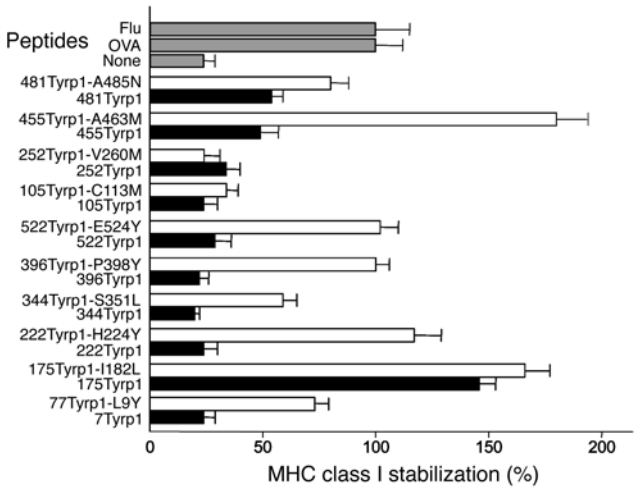

Figure 1
Rational optimization of peptide anchor residues in mouse Tyrp1 enhances MHC class I binding. Tyrp1-optimized peptides (white bars) and their wild-type counterparts (black bars) were assessed for MHC class I stabilization in assays using RMA-S cells. Results are expressed as percentage of MHC class I stabilization relative to OVA and influenza (Flu) peptides. Experiments were performed twice in triplicate with identical results; error bars represent standard deviation of the mean.

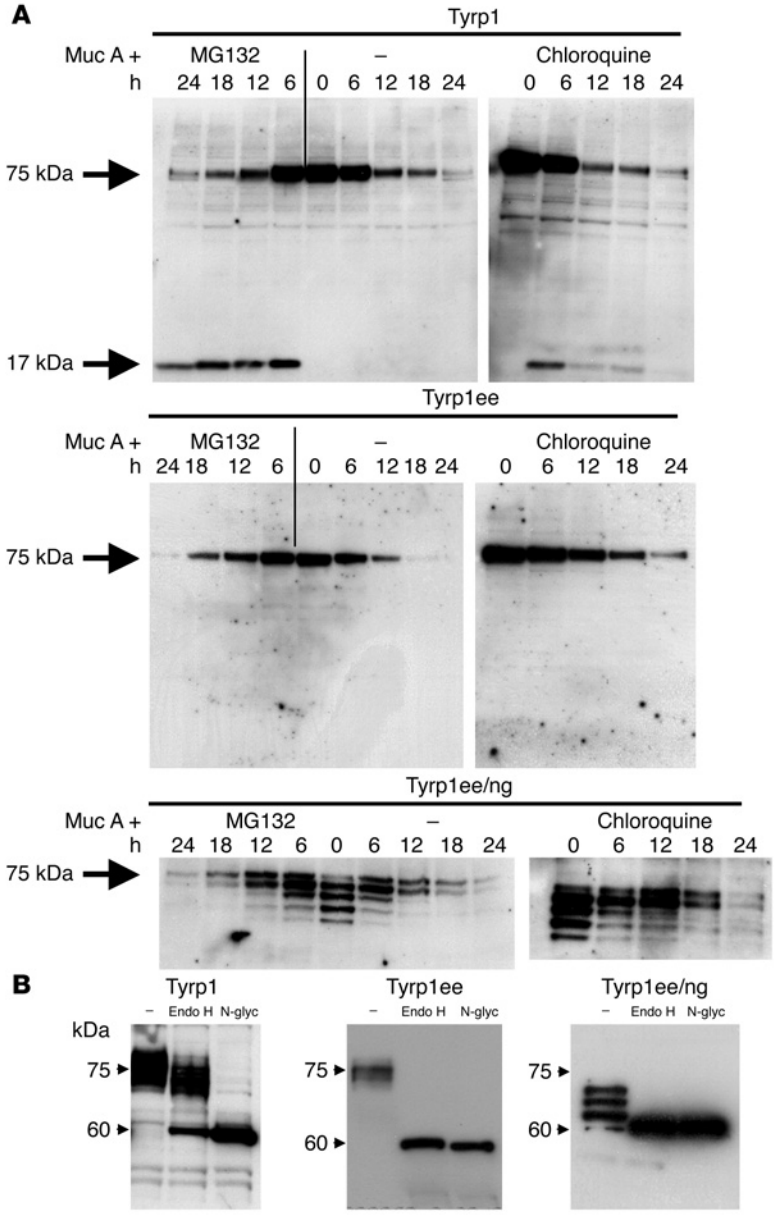

Figure 2

Biosynthesis and stability of wild-type Tyrp1, Tyrp1ee, and Tyrp1ee/ng. Biosynthesis was assessed by transfection of Cos-7 cells with plasmid DNA encoding Tyrp1 constructs. Each Tyrp1 construct was Flag-tagged at the carboxyl terminus. (**A**) At 24 hours after transfection, cells were treated with muconomycin A (Muc A) to inhibit protein synthesis and chased for an additional 24 hours in the presence of inhibitors (MG132 or chloroquine) or without inhibitors. The 0 time point corresponds to 24 hours after initial transfection, and 6, 12, 18, and 24 are the hours of chase after the 0 time point. (**B**) Digestion of high mannose carbohydrate moieties with Endo H or all Asn-linked sugars with N-glycanase (N-glyc) for Tyrp1, Tyrp1ee, and Tyrp1ee/ng.

that increased in intensity over the 6-hour chase (Figure 2A). These results were reproduced in 3 different experiments for wild-type Tyrp1 and Tyrp1ee and 4 experiments for Tyrp1ee/ng.

Deficient maturation of carbohydrate moieties on Tyrp1ee and Tyrp1ee/ng. Although the Tyrp1ee/ng ladder might represent intermediate degradation products, particularly because glycosylation sites had been mutated, we suspected that the ladder instead represented different unstable glycosylated forms of Tyrp1 based on a close resemblance to our prior results with partial digestion of Tyrp1 by N-glycanase (33). Digestion with the enzymes endoglycosidase H (Endo H) and N-glycanase collapsed the ladder to a single band of approximately 59–60 kDa (Figure 2B). These results show that sugars on Tyrp1ee/ng were not processed beyond the ER (based on Endo H sensitivity), with the ladder representing different glycosylated polypeptides of Tyrp1ee/ng. Thus Asn→Gln conversion did not completely abrogate glycosylation, but rather created a series of ER-retained, differentially glycosylated polypeptides (with glycans at 0, 1, 2, 3, or 4 Asn sites). The highest-mass 75-kDa band, which increased over 6 hours, was consistent with further posttranslational processing. In addition, Tyrp1ee glycans were also sensitive to Endo H, showing that the mutations in Tyrp1ee led to ER retention — probably through misfolding — with no further processing in the Golgi, followed by proteasome degradation (shown below; Figure 2B).

Tyrp1ee/ng mutants are degraded in a proteasome-dependent pathway. Protein stability and degradation of wild-type Tyrp1, as assessed over a 24-hour chase, were nearly identical to what we have previously reported in mouse melanocytic cells, consistent with little or no effect of the Flag tag or expression in Cos-7 cells on stability or degradation (33, 35, 39) (Figure 2A). We investigated the effects of chloroquine (to inhibit degradation in acidic compartments) and the proteasome inhibitor MG132. The fate of mature wild-type Tyrp1 was minimally affected by either inhibitor (Figure 2A). A short-lived 17-kDa carboxyterminal degradation fragment of wild-type Tyrp1 was detected in the presence of inhibitors but was not detected for Tyrp1ee and Tyrp1ng.

The stability of Tyrp1ee was essentially the same as for wild-type Tyrp1, despite ER retention. The majority of Tyrp1ee underwent proteasome degradation, with a minor proportion reaching acidic compartments for delayed degradation (Figure 2A). Thus the mutations in Tyrp1ee altered its trafficking, leading to ER retention and proteasome degradation.

Total degradation of Tyrp1ee/ng was modestly delayed by proteasome inhibition over 12 hours (Figure 2A). When higher and lower Tyrp1ee/ng bands were examined, the higher-mass glycoforms (~75 and 69 kDa) were less stable than wild-type Tyrp1 and were degraded largely via acidic compartments, presumably the endosomal pathway (Figure 2A). The 3 lower-mass forms (~65–66, 61–63, and 59–60 kDa, representing glycoforms with 1 or 2 carbohydrate moieties and the naked polypeptide) were very unstable, retained in the ER, and not rescued by either proteasome inhibition or chloroquine (Figure 2A). In summary, Tyrp1ee/ng generates multiple unstable products that are degraded both in the endosomal pathway (high-mass forms) and through proteasomes (low-mass forms).

Increased immunogenicity of Tyrp1ee mutants. Although candidate altered peptide ligands of Tyrp1ee had enhanced binding to MHC class I (Figure 1), we needed to ascertain whether these epitopes could be naturally processed and presented. To increase immuno-

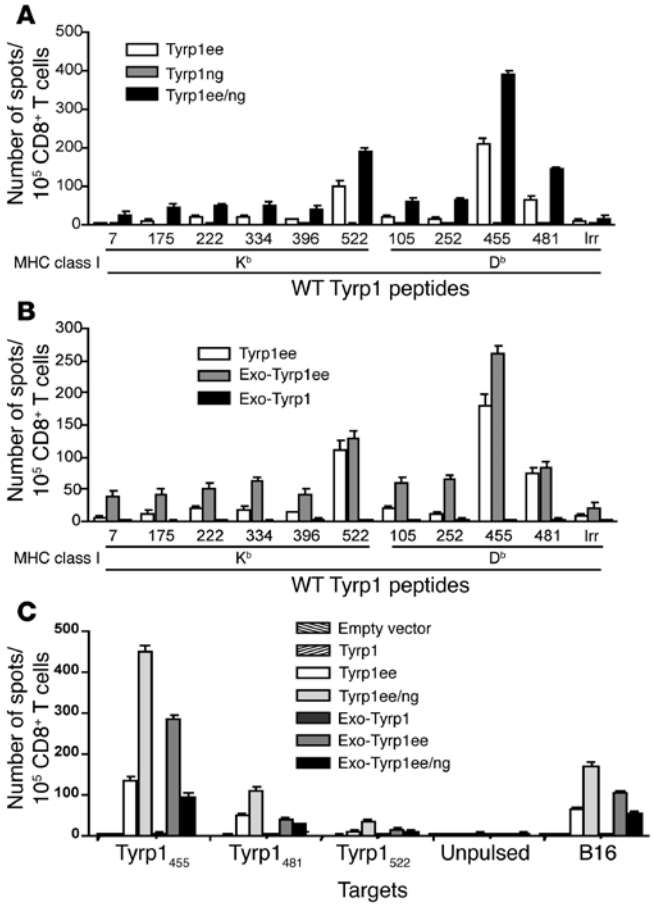

Figure 3
Immunization with optimized Tyrp1 induces epitope-specific CD8+ T cell responses. C57BL/6 mice (5 per group) were immunized once weekly for 4 weeks with DNA encoding empty control vector, Tyrp1, Tyrp1ee, Tyrp1ng, Tyrp1ee/ng, exo-Tyrp1, exo-Tyrp1ee, or exo-Tyrp1ee/ng. CD8+ T cells were purified, and IFN-γ secretion was evaluated in ELISPOT assays after overnight stimulation with the designated peptide, B16 melanoma cells, or EL-4 target cells loaded with designated wild-type Tyrp1 peptides. ELISPOT assay results (IFN-γ secretion) are shown as number of spots per 10^5 CD8+ T cells. Experimental results were reproduced 3 times, each time in triplicate; error bars represent standard deviation of the mean. (**A** and **C**) Removal of Asn glycosylation sites resulted in enhanced immunogenicity of Tyrp1ee. (**B** and **C**) Incorporating the exotoxin A domain increased immunogenicity of Tyrp1ee but decreased immunogenicity of Tyrp1ee/ng. (**C**) Comparison of CD8+ T cell responses after immunization with all Tyrp1 constructs.

genicity further, Tyrp1 mutants were ligated to the translocation domain of *Pseudomonas aeruginosa*'s exotoxin A, which enhances CD8+ T cell responses in other immunization models (40–42). The exotoxin A domain was fused upstream of Tyrp1 (exo-Tyrp1), Tyrp1ee (exo-Tyrp1ee), and Tyrp1ee/ng (exo-Tyrp1ee/ng); alternatively, exotoxin A alone was noncovalently mixed with Tyrp1ee. Immunogenicity was initially addressed by assessing the ability of immunization with DNA constructs encoding full-length wild-type or mutated Tyrp1 constructs to induce CD8+ T cell responses against wild-type Tyrp1 peptides in C57BL/6 mice. Mice were immunized with 4 μg DNA 4 times by ballistic bombardment (14). Purified CD8+ T cells were tested for IFN-γ secretion in ELISPOT assays after 18-hour stimulations to detect responses to wild-type Tyrp1 epitopes and to intact syngeneic melanoma cells.

Immunization with wild-type Tyrp1, exo-Tyrp1, and Tyrp1ng did not induce any detectable T cell response, but CD8+ T cell responses were seen in mice immunized with Tyrp1ee, Tyrp1ee/ng, exo-Tyrp1ee, and exo-Tyrp1ee/ng (Figure 3, A–C). Immunization with Tyrp1ee induced responses against 3 wild-type Tyrp1 peptides, 455, 481, and 522 (Figure 3, A and C). We believe these to be novel MHC class I–restricted Tyrp1 epitopes revealed by this DNA immunization strategy. Immunization with Tyrp1ee/ng induced a substantially higher CD8+ T cell response against peptides 455, 481, and 522, increasing responses by 70%, 90%, and 95%, respectively, compared with Tyrp1ee (Figure 3A).

Exo-Tyrp1ee elicited higher CD8+ responses than did Tyrp1ee against peptide 455 (Figure 3, B and C). However, fusion of the exotoxin A domain into Tyrp1ee/ng substantially diminished its potency down to Tyrp1ee levels (Figure 3C). Notably, CD8+ T cells primed by immunization with Tyrp1ee, Tyrp1ee/ng, exo-Tyrp1ee, and exo-Tyrp1ee/ng were able to respond to intact B16 melanoma cells, with Tyrp1ee/ng and Tyrp1ee eliciting the strongest response and exo-Tyrp1ee/ng the lowest (Figure 3C). Immunization with DNA encoding the exotoxin A fragment mixed with Tyrp1ee DNA showed no enhancement of CD8+ T cell responses compared with Tyrp1ee immunization alone (data not shown), indicating that the effect of exotoxin A is not mediated simply through the expression of exotoxin A (e.g., exotoxin helper epitopes). These results demonstrate that Tyrp1ee, Tyrp1ee/ng, exo-Tyrp1ee, and exo-Tyrp1ee/ng generated strong functional CD8+ T cell responses that recognized naturally processed and presented Tyrp1 epitopes expressed by B16 melanoma. Through this approach, we identified what we believe to be novel CD8+ T cell epitopes in a tissue self antigen, demonstrating a proof of concept for discovery of subdominant and cryptic epitopes in self antigens that can be processed and presented.

Antitumor effects following immunization with optimized DNA. To investigate the in vivo effects of these rationally designed Tyrp1 DNA constructs, we assessed their ability to protect mice against lethal challenge with B16 melanoma cells. Palpable intradermal tumors were detected between days 4 and 8 following B16 challenge in naive mice with a tumor challenge that was 50- to 100-fold greater than the minimum lethal dose. No delay was observed in mice immunized with Tyrp1, Tyrp1ng, or exo-Tyrp1 (Figure 4A; Tyrp1ng data not shown). Notably, tumor protection was observed in approximately 40–45% of mice immunized with Tyrp1ee ($P < 0.05$, log-rank analysis) and 75–90% of mice immunized with Tyrp1ee/ng ($P < 0.001$; Figure 4A), with the same results observed in 4 independent experiments. Immunization with exo-Tyrp1ee and Tyrp1ee/ng led to greater tumor protection compared with Tyrp1ee (~40–45% to ~75–90%; $P < 0.001$; Figure 4, A and B). Ligating exotoxin A to Tyrp1ee/ng substantially diminished antitumor effects to below 20% tumor protection (Figure 4A), and mixing Tyrp1ee with exotoxin A showed no enhancement of tumor immunity (Figure 4B). These results demonstrated the effectiveness of immunization with epitope-enriched self antigens and revealed increased potency when the self antigen was further destabilized by modifying glycosylation and conjugating to exotoxin A.

Autoimmunity manifested as patchy coat hypopigmentation was observed in 42 of the 45 mice immunized with Tyrp1ee, Tyrp1ee/ng, exo-Tyrp1ee, and exo-Tyrp1ee/ng, but in none of the 30 mice immunized with wild-type Tyrp1, in 3 experiments (data not shown). The most marked hypopigmentation was observed in mice immunized

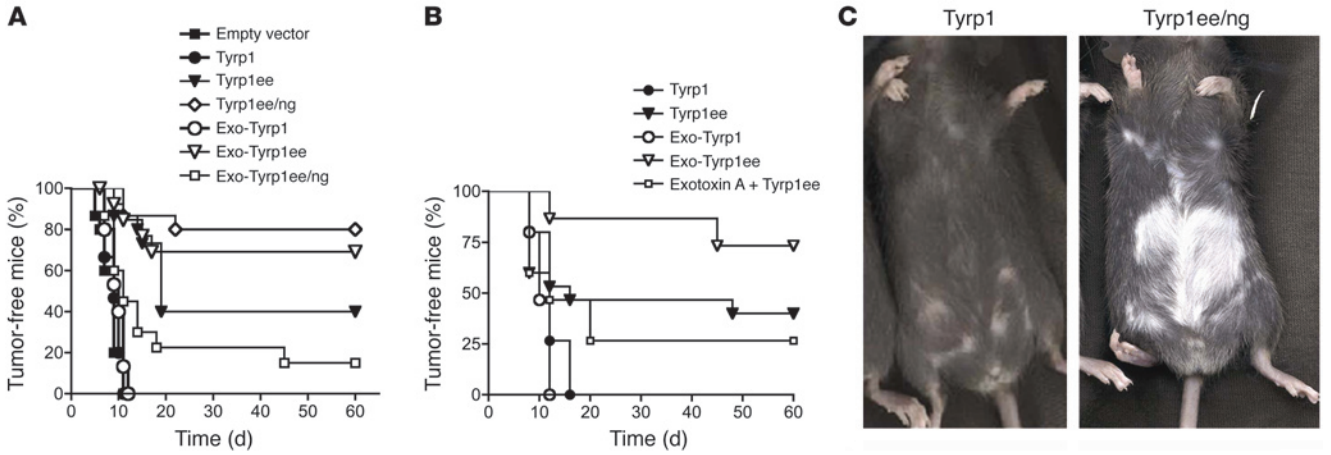

Figure 4
Immunization with optimized Tyrp1 rejects tumors and induces autoimmunity. C57BL/6 mice (15 per group) were immunized once weekly for 4 weeks (unless otherwise indicated in Methods) with Tyrp1, Tyrp1ee, Tyrp1ee/ng, Tyrp1ng, exo-Tyrp1, exo-Tyrp1ee, exo-Tyrp1ee/ng, and exotoxin A vector plus Tyrp1ee separately. Kaplan-Meier analyses are shown. (**A**) Immunization with exo-Tyrp1ee and -Tyrp1ee/ng protected ~75–90% ($P < 0.01$) of mice challenged with B16 melanoma cells, whereas Tyrp1ee immunization induced partial protection of ~40% ($P < 0.05$) and exo-Tyrp1ee/ng decreased protection (~10%). (**B**) Immunization with exo-Tyrp1ee DNA protected ~75% of mice and increased tumor protection compared with Tyrp1ee or exotoxin A plus Tyrp1ee ($P < 0.05$ versus Tyrp1). (**C**) Tyrp1ee/ng-induced autoimmunity manifested as coat hypopigmentation. Representative mice immunized with either Tyrp1ee/ng or Tyrp1 are shown.

with Tyrp1ee/ng, with a representative mouse shown in Figure 4C. Mice with autoimmune hypopigmentation after surviving tumor challenge remained otherwise healthy for up to 12 months or more.

Immunity induced by optimized Tyrp1 vaccines is CD8 dependent. Tumor immunity was completely abrogated in mice immunized with Tyrp1ee, exo-Tyrp1ee, and Tyrp1ee/ng following depletion of $CD8^+$ T cells, but not with depletion of $CD4^+$ cells or NK cells (Figure 5, A–C); to our knowledge, no difference in tumor-free survival in mice immunized with wild-type Tyrp1 with or without $CD8^+$ depletion has been previously reported (14). These results showed that the immune responses induced by the optimized vaccines were CD8 dependent, without a requirement for $CD4^+$ or NK cells for tumor rejection.

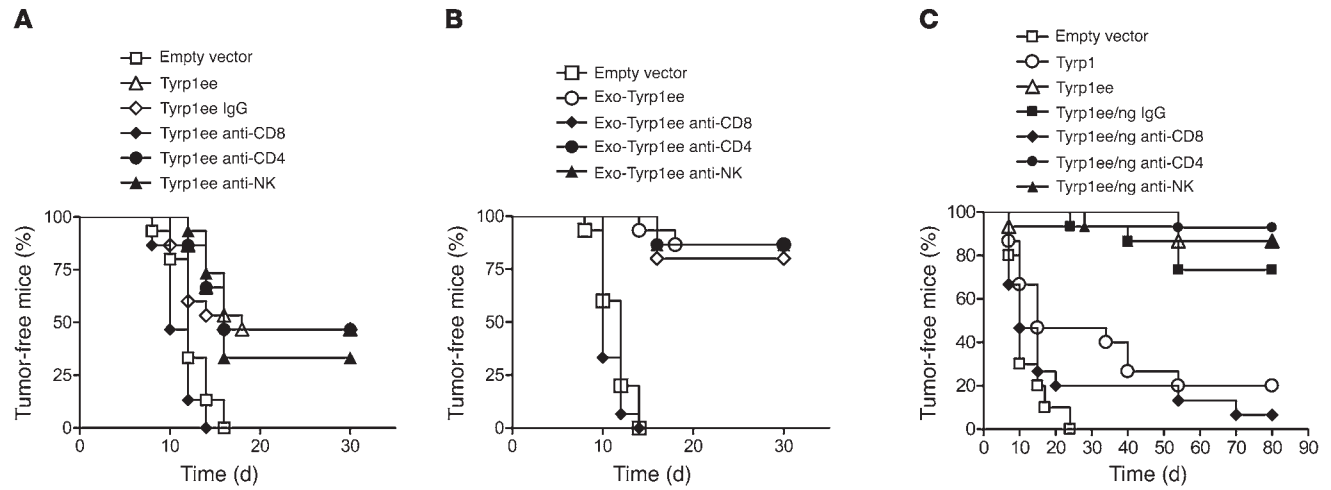

Figure 5
Immunization with Tyrp1ee, exo-Tyrp1ee, and Tyrp1ee/ng protects mice from tumor challenge through a mechanism dependent on $CD8^+$ T cells. C57BL/6 mice (15 per group) were immunized once weekly for 4 weeks with different Tyrp1 constructs. Five days after the last vaccination, mice were challenged intradermally with 10^5 B16 melanoma cells. $CD8^+$, $CD4^+$, and NK cells were depleted by weekly intraperitoneal injection of 500 μg anti-CD8 (53.6-72), anti-CD4 (GK1.5), or anti-NK (PK-136) administered 3 days before starting immunization. Depleting antibodies were subsequently administrated every week for the duration of the experiment. Rat monoclonal IgG was administered as a control. Kaplan-Meier analyses are shown. (**A**) Immunization with Tyrp1ee DNA protected ~45% of mice challenged with B16 melanoma ($P < 0.01$) compared with mice vaccinated with the control (empty vector). Tumor protection was completely abrogated in mice depleted of $CD8^+$ T cells, but neither CD4 nor NK cell depletion significantly affected tumor protection induced by immunization with Tyrp1ee. (**B**) Immunization with exo-Tyrp1ee DNA protected ~80% of mice ($P < 0.05$) compared with empty vector and was completely abrogated in mice depleted of $CD8^+$ T cells. No significant decreases in tumor protection were observed in mice vaccinated with exo-Tyrp1ee and depleted of CD4 and NK cells. (**C**) Immunization with Tyrp1ee/ng conferred increased tumor protection (~70%) ($P < 0.05$ compared with empty vector or Tyrp1), which was completely dependent of $CD8^+$ T cells.

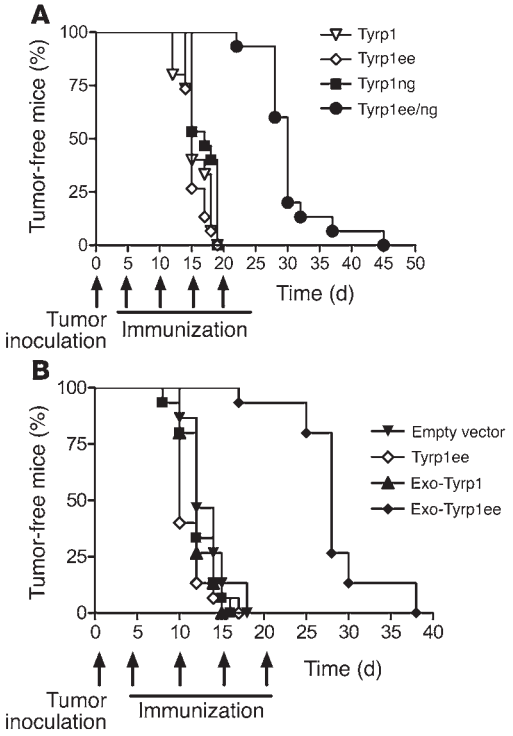

Figure 6
Immunization with Tyrp1ee/ng and exo-Tyrp1ee significantly prolongs tumor-free survival in a treatment model. C57BL/6 mice (15 per group) were left untreated or were treated every 5 days for 4 immunizations with empty vector, Tyrp1, Tyrp1ee, Tyrp1ng, Tyrp1ee/ng, exo-Tyrp1, or exo-Tyrp1ee starting 4 days after the challenge with 10^5 B16 melanoma cells. Tumor growth was monitored every 2 days. Tumor-free survival was significantly delayed in mice immunized with (**A**) Tyrp1ee/ng ($P < 0.0001$ versus Tyrp1 immunization) and (**B**) exo-Tyrp1ee ($P < 0.001$ versus empty vector and Tyrp1 immunization).

Immunization with optimized Tyrp1 vaccines in a treatment model. Immunization with optimized Tyrp1 constructs was examined in a treatment model by initiating immunization 4 days after challenge with B16 cells. Significant delays in tumor growth and prolonged survival were observed in mice treated with Tyrp1ee/ng ($P < 0.05$; Figure 6A) and exo-Tyrp1ee ($P < 0.01$; Figure 6B). No treatment effects were detected in mice immunized with Tyrp1ee, exo-Tyrp1, or Tyrp1.

*Epitope optimization for HLA-A*0201.* To design a vaccine that might be clinically applied to people with melanoma, an epitope-enriched mouse Tyrp1 DNA construct (Tyrp1ee/A*0201) was created. This construct contained 6 mutations optimized for HLA-A*0201 binding within polypeptide regions that are highly conserved between mouse and human Tyrp1. HLA-A*0201/K^b transgenic mice (43) were immunized with plasmid DNA encoding wild-type Tyrp1 or Tyrp1ee/A*0201. Purified $CD8^+$ T cells from immunized mice were assessed for responses to Tyrp1 epitopes by secretion of IFN-γ following stimulation with either TAP2-deficient T2 cells or HLA-negative K562 cells transfected with HLA-A*0201 (44) and pulsed with wild-type Tyrp1 peptides. Strong $CD8^+$ T cell responses against 2 wild-type Tyrp1 peptides, 188–196 and 213–221, were detected only in mice immunized with Tyrp1ee/A*0201 (Figure 7A). $CD8^+$ T cells against wild-type Tyrp1 peptide 213–221 responded to HLA-A*0201–positive, but not –negative, human melanoma cells, supporting processing and presentation of the 213–221 epitope by human melanoma cells (Figure 7, B and C). $CD8^+$ T cells against the Tyrp1 peptide 188–196 reacted with HLA-A*0201–positive melanoma cells but also responded weakly to HLA-A*0201–negative melanoma cells, making inferences about HLA-restricted processing and presentation for this epitope more difficult (data not shown). Of note, HLA-A*0201 transgenic mice express the mouse heavy chain α3 domain, while HLA-A*0201 molecules expressed by T2 and transfected K562 cells contain only the human heavy chain α3 domain, suggesting that newly generated Tyrp1-specific $CD8^+$ T cells have high avidity because they respond independently of CD8 coengagement (45, 46).

Discussion

In this study we showed how altered ligands for MHC introduced into DNA encoding a tissue-specific self antigen led to multivalent T cell responses against that self antigen and also identified what we believe to be novel epitopes. We adapted the strategy to identify a HLA-A*0201–restricted Tyrp1 epitope that can be evaluated for clinical use in the future. Rationally altering individual MHC anchor residues not only can enhance MHC binding, but can also reposition solvent-facing residues for binding to CDR3 regions of T cell receptors for increased T cell activation (47, 48). We showed that these types of mutations also altered protein trafficking, leading to ER retention and enhancing availability of degradation products for processing by proteasomes.

Immunogenicity was further enhanced by creating different Tyrp1 glycoforms carrying mutations at Asn glycosylation sites to improve antigen processing and presentation. Sugars play roles both in protein folding and in protection from degradation by proteases. Notably, the Asn→Gln conversion still allowed inefficient glycosylation, creating isoforms with different numbers of carbohydrates. These glycosylation-deficient products included underglycosylated isoforms that were rapidly degraded for proteasome processing. In particular, glycoforms with 1 and 2 carbohydrate residues, along with the naked polypeptide, were rapidly degraded through a proteasome-dependent pathway. Immunity was greatest when mutations for altered peptides and glycosylation were combined.

Because Asn-linked glycosylation sites are highly conserved among members of the tyrosinase family (34), this optimization strategy should be applicable to other melanoma antigens. Furthermore, our studies have relevance to the design of optimized versions of other tissue-specific differentiation glycoproteins, overexpressed glycoproteins, and subdominant glycoprotein antigens of pathogens.

For self glycoproteins, immunization carries the risk of autoimmunity, which limits this approach when the target antigen is expressed by critical tissues. However, target antigens restricted to nonvital cell types and tissues such as melanocytes, prostate epithelium, or breast ductal epithelium are candidates for this strategy. A number of mouse studies have shown that autoimmune vitiligo is tolerated well when tumor immunity is induced against tyrosinase family antigens and that development of vitiligo is associated with improved response to therapy and outcome in patients with melanoma (reviewed in 1, 2, 13–16).

Prior reports in viral models and clinical observations have suggested that narrow T cell responses against individual epitopes can lead to persistence of virus, while broader responses are associated with control or resolution of infection (49–53). By using the strategy reported here, broader T cell responses against multiple epitopes can be generated with possible advantages, including a

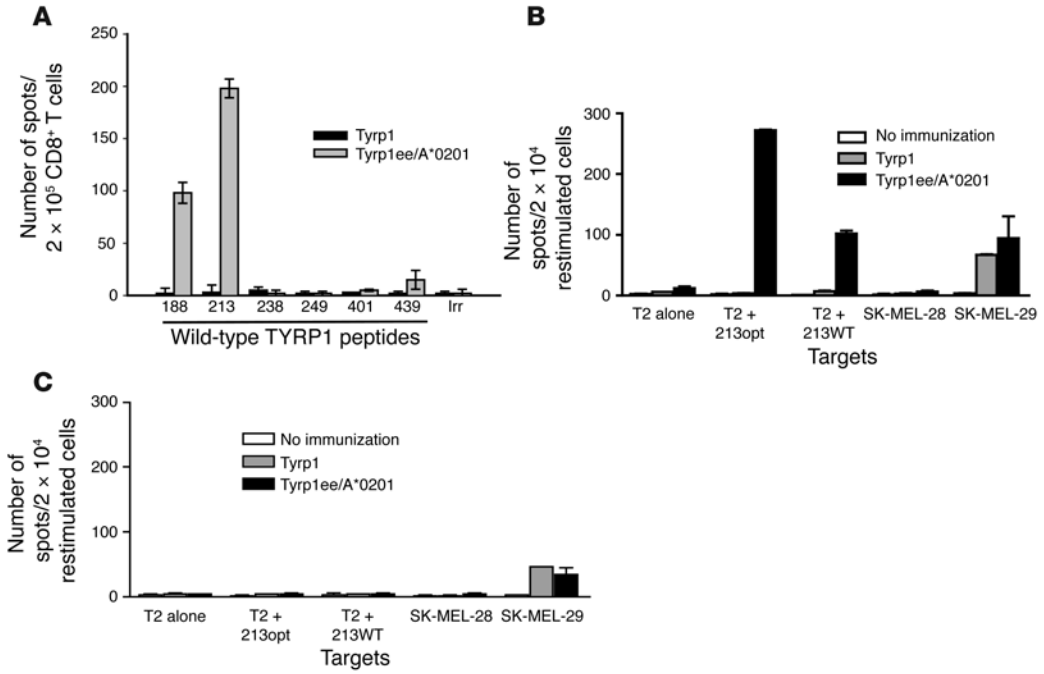

Figure 7
Immunization with optimized Tyrp1 induces HLA-A*0201–restricted $CD8^+$ T cells against Tyrp1. $CD8^+$ T cells were purified from transgenic HLA-A*0201/K^b mice immunized 4 times weekly with plasmid DNA encoding Tyrp1 or Tyrp1ee/A*0201. (**A**) $CD8^+$ T cells were assessed for response to wild-type Tyrp1 peptides (see Table 1) using K562/HLA-A*0201 cells as APCs in 20-hour ELISPOT assays. Irr, irrelevant peptide. (**B** and **C**) $CD8^+$ T cells were restimulated for 7 days with T2 cells pulsed with the wild-type $Tyrp1_{213}$ peptide (**B**) or no peptide (**C**) and assayed by ELISPOT for response to wild-type (WT) or optimized (opt) $Tyrp1_{213}$ peptide pulsed on T2 cells or to HLA-A*0201–positive (SK-MEL-29) and –negative (SK-MEL-28) human melanoma cells. Experiments were reproduced 3 times in triplicate; error bars represent standard deviation of the mean.

decreased likelihood of mutated tumor escape variants that might occur with altered ligands created with single amino acid substitutions (54). Thus we propose that the breadth and diversity of T cell responses is also important for cancer immunity (49).

Overall, our results indicate that it is the combined effect of epitope optimization, enrichment for multiple epitopes, and enhanced processing that leads to increased efficacy of immunization. The underlying mechanisms involved both facilitated processing and enhanced pMHC stability (with probable increased T cell activation). Thus multiple steps in the pathway to final antigen presentation can be manipulated to make multivalent vaccines. These observations provide broader strategies that can be applied to guide specificity of T cell responses in treatment with cytokines, cytotoxic T lymphocyte–associated antigen 4 blockade, recovering T cell homeostasis, and other nonspecific strategies known to generate cancer immunity and tumor rejection (25).

Methods

Mice. Female C57BL/6 mice were purchased from the National Cancer Institute breeding program. HLA-A*0201/K^b were obtained from L. Sherman (Scripps Institute, La Jolla, California, USA; ref. 55). These mice were intercrossed and phenotyped for HLA-A*0201 expression by flow cytometry. All mice used in experiments were between 8 and 10 weeks of age. Care and use of these mice was in accordance with institutional guidelines under a protocol reviewed and approved by the Institutional Animal Care and Use Committee of Memorial Sloan-Kettering Cancer Center (MSKCC).

Antibodies. The anti-CD8 mAb 53.6-72 (rat IgG) was obtained from the American Type Culture Collection. The anti-CD4 mAb (Gk1.5) and anti-NK mAb (PK136) were obtained from the MSKCC Monoclonal Antibody Core Facility. Flow cytometry and the MHC class I stabilization assays were performed as previously described (29) using a FACScan instrument equipped with Lysis II software (BD).

Peptides. The Tyrp1 peptides used in this study (Table 1), $OVA_{25–264}$ (SIINFEKL, K^b-restricted) and influenza virus $nucleoprotein_{366–374}$ (ASNENMETM, D^b-restricted), were synthesized by GeneMed Synthesis Inc. and purified by HPLC to >80% purity. They were resuspended in 100% DMSO at a concentration of 40 mg/ml, diluted with PBS (final concentration, 2 mg/ml), and then frozen in aliquots at –20°C.

Plasmid constructs and site-directed mutagenesis. The mouse *Tyrp1* cDNA was mutated using reiterations of the Quickchange protocol (Stratagene). Bulk plasmid miniprep from each round of mutagenesis was used as template for the next. Candidate clones for each construct were sequenced after the last round. A unique *AscI* restriction site was inserted into pCDNA3.1(+) (Invitrogen Corp.) by cloning an oligonucleotide duplex in the *NotI* site of the polylinker 5′-GGCCTGGCGCGCCGTACGTTAACATCGATGC-3′ (upper strand) and 5′-GGCCGCATCGATGTTAACGTACGGCGCGCCA-3′ (lower strand). The new polylinker was then subcloned into pCR3 (Invitrogen Corp.) as a *HindIII-XbaI* fragment, yielding the pCRAN expression vector. All inserts described in the following paragraphs were confirmed by DNA sequencing and subcloned into the pCRAN vector.

For construction of Tyrp1ee, the following oligonucleotides were used (mutant bases are underlined): L9Y, 5′-CGTCCTCCCCTAC-GCCTATATCTCC-3′; C113M, 5′-CTGTGGGACTATGCGTCCTGGGTGG-3′; I182L, 5′-CCAAATTTGAGAACCTGTCCGTTTATAACTACTTTG-3′; H224Y, 5′-GCTTTTCTCACATGGTACAGGTACCATCTGCTG-3′; V260M, 5′-GTCTGCGATATGTGCACTGATGACTTGATGGG-3′; S351L, 5′-CCTCCTTTTTATTCCAATCTGACAGACAGTTTTCGAAATACAGTG-3′; P398Y, 5′-CCCATTTGTCTCCCAATGATTACATTTTTGTCCTCCTGCA-CAC-3′; A463M, 5′-CCAGACAATCTGGGATATATGTATGAAGTTCAAT-GGCCAGG-3′; A485N, 5′-CCATTGCTGTAGTGAACGCGTTGTTACTTGTAGCTGCC-3′; E524Y, 5′-CACTATCAACGCTATGCTTACGACTATGAGGAGCTC-3′.

The Tyrp1ng mutant was created by Asn→Gln mutations at amino acid positions 96, 104, 181, 304, 350, and 385 using the following primers (only sense primers are shown): N96Q, CCTGGCCTCTGAG-GTTCTTTCAGAGAACATGTCAGTGCAATG; N104Q, GAACATGT-CAGTGCAATGATCAGTTCTCAGGACACAACTGTG; N181Q, GCAA-

CACACCACAATTTGAGCAGATTTCCGTTTATAACTACTTTG; N304Q, CCCTGGGAACACTTTGTCAGAGCACTGAGGGTGGACC; N350Q, GACACACCTCCTTTTTATTCCCAGTCTACAGACAGTTTTCG; N385Q, CCTGGCCCACCTCTTCCTGCAGGGAACGGGAGG.

These same primers were used to create Asn→Gln mutations in Tyrp1ee to generate Tyrp1ee/ng, which contained both potential altered peptide ligands and deficient glycosylation sites. For creation of Tyrp1/HLA-A*0201, the following primers were used: Tyrp1–188-A2.1 CATTTCCGTTTATAACTACTTTCTGTGGACACACTATTATTCAG; Tyrp1–213-A2.1, CTTTGGGGATGTGGATTTCCTGCACGAAGGACCCGCTTTTC; Tyrp1–238-A2.1, GGAGAGAGACATGCAGGAGTACCTGCAGGAGCCTTCTTTC; Tyrp1–249-A2.1, CTCCCTTCCTTACTGGCTGTTTGCAACTGGGAAAAACGTC; Tyrp1–401-A2.1, GCACACTTTCACTGATGTGGTCTTTGACGAATGGC; Tyrp1–439-A2.1, GACATAACAGGCAATACTACATGGTGCCATTCTGG.

The *P. aeruginosa* exotoxin A fusion vector was created as follows: genomic DNA from *P. aeruginosa* (American Type Culture Collection) was extracted using the DNeasy kit (QIAGEN). A fragment encoding the first 404 amino acids of exotoxin A (including signal peptide) was amplified by PCR using the following primers: sense (start codon underlined; *HindIII* site italicized), 5′-TTT*AAGCTT*CCACCATGCACCTGATACCCCATTG-3′; antisense (*AscI* site italicized), 5′-A*GGCGCGCCC*CGCATTCACCGGCGGCGAC-3′. The PCR product was cloned as a *HindIII-AscI* fragment into pCRAN, yielding the pCT5 expression vector, in which exotoxin was upstream (aminoterminal) from the Tyrp1 sequence of interest. Wild-type and mutant versions of *Tyrp1* cDNA were flanked by *AscI* (upstream) and *NotI* (downstream) sites. These restriction sites were used for subcloning into pCRAN, yielding the Tyrp1 and Tyrp1ee constructs, or pCT5, yielding the exo-Tyrp1 and exo-Tyrp1ee constructs. The amino acid sequence at the in-frame junction with exotoxin was AGECGRAT**M** (Cys 404 of exotoxin underlined; Met 1 of Tyrp1 in bold).

Transfection experiments. To introduce a FLAG tag at the carboxyl terminus of Tyrp1 and its variants, cDNAs were reamplified by PCR using a downstream primer that omits the normal Stop codon and cloned between the *EcoRV* and *SalI* sites of the pCMV-Tag4A vector (Stratagene). The upstream primer was GGCGCGCCACCATGAAATCTTACAACGTCC, and the downstream primer was ATTCATAGTCGACGACCATGGAGTGGTTAGGATTC.

COS-7 cells ($1–2 \times 10^6$) were transfected with each FLAG-tagged Tyrp1 variant using the Fugene 6 reagent (Roche Diagnostics Corp.). At 24 hours after transfection, cells were treated for 1 hour with muconomyin A (0.6 μM; Sigma-Aldrich). Following washes, culture was prolonged either without further treatment or in the presence of the proteasome inhibitor MG132 (20 μM; Sigma-Aldrich) or chloroquine (50 μM). Cells were washed in PBS and lysed in 12.5 mM Tris (pH 7.5), 1.25% Triton X-100, and 190 mM NaCl for 30 minutes on ice. Cell lysates were normalized for protein content and analyzed by SDS-PAGE and Western blotting using peroxidase-conjugated M2 anti-FLAG mAb (Sigma-Aldrich).

Immunizations. Genetic immunization using DNA-coated gold particles was performed using a gene gun provided by PowderMed Ltd. as previously described (14, 18). Four injections (400 pounds/inch^2) were delivered to each mouse, one to each of the abdominal quadrants, for a total of 4 μg plasmid DNA per mouse per week for 4 weeks.

IFN-γ ELISPOT assay. IP-Multiscreen plates (Millipore) were coated with 100 μl anti-mouse IFN-γ antibody (10 μg/ml; clone AN18; Mabtech) in PBS and incubated overnight at 4°C. After washing with PBS to remove unbound antibody, plates were blocked with RPMI containing 7% fetal bovine serum for 2 hours at 37°C. Purified CD8$^+$ T cells were plated at a concentration of 10^5 cells/well. For antigen presentation, 5×10^4 irradiated EL-4 cells, T2 lymphoma cells, or HLA-A*0201/K562 cells pulsed with 10 μg/ml peptide were added to a final volume of 100 μl/well. After incubation for 20 hours (EL-4 or HLA-A*0201/K562 cells) or 7 days (T2 cells) at 37°C, plates were extensively washed with PBS plus 0.05% Tween and incubated with 100 μl/well of biotinylated antibody against mouse IFN-γ (2 μg/ml; clone R4-6A2; Mabtech). Plates were incubated for an additional 2 hours at 37°C, and spot development was performed as described (56). Spots were counted with an Automated ELISPOT Reader System with KS software (version 4.3; Carl Zeiss Inc.) by an independent investigator in a blinded fashion.

Tumor challenge. These experiments were carried out with B16 melanoma cells as described previously (18). Prophylactic and therapeutic effects of the vaccine were determined by intradermally challenging mice with 10^5 and 3×10^4 B16F10 melanoma cells, respectively. Cells were injected into the shaved right flank of each mouse. Tumor growth was monitored at least 3 times per week, initially by palpation only and subsequently using Vernier calipers when tumors were palpated. Mice surviving tumor challenge were followed for a minimum of 40–100 days. If maximum tumor diameter reached 10 mm, the tumor became ulcerated, or mice showed discomfort, mice were euthanized. Tumor-free survival was plotted by Kaplan-Meier plots and compared by log-rank analysis.

Depletion of CD8$^+$, CD4$^+$, and NK cells. Depletion of CD8$^+$ T cells, CD4$^+$ T cells, and NK cells in vivo was performed by intraperitoneal injections (3 days before starting immunization and then weekly for the remainder of the experiment) with 500 μg/injection of 53.6-72 rat anti-mouse mAb, Gk1.5 mAb, and PK136 mAb, respectively. Depletion of CD8$^+$ T cells (≥93%), CD4$^+$ T cells (≥94%), and NK cells (≥97%) was confirmed by fluorescence-activated cell sorting analysis of peripheral blood.

Endo H and N-glycanase analysis. Lysates of 2×10^4 COS-7 cells receiving no inhibitor treatment were digested 24 hours after transfection for 5 hours with 0.005 U Endo H or N-glycanase (Sigma-Aldrich) at 37°C. Samples were analyzed by SDS-PAGE as we have previously described (34, 35, 39).

Statistics. Tumor-free survival was plotted using the Kaplan-Meier method, and statistical significance was determined by log-rank analysis. Differences were considered significant at $P < 0.05$.

Acknowledgments

Support for this work was provided by NIH grants R01 CA56821, P01 CA33049, and P01 CA59350 (to A.N. Houghton); Swim Across America; the Mr. William H. Goodwin and Mrs. Alice Goodwin and the Commonwealth Cancer Foundation for Research and the Experimental Therapeutics Center of MSKCC (to A.N. Houghton, J.A. Guevara-Patiño, M.E. Engelhorn); NIH training grant T32 CA09149 (to M.J. Turk); and a Fellowship award from the Cancer Research Institute (to M.E. Engelhorn). J.D. Wolchok is supported by a Damon Runyon/Eli Lilly Award, and A.N. Houghton has Damon Runyon/Eli Lilly mentorship support. We are extremely grateful to the Annenberg Hazen Foundation as well as to the Louis & Anne Abrons Foundation, the T.J. Martell Foundation, the Peter J. Sharp Foundation/Breast Cancer Research Foundation, and the Mr. and Mrs. Quentin J. Kennedy Fund. We thank David Posnett and Lisa Denzin for helpful comments, Rodica Stan for invaluable assistance in preparing the manuscript, and Linda Sherman for providing the HLA-A*0201/K^b mice.

Received for publication May 9, 2005, and accepted in revised form February 21, 2006.

Address correspondence to: José A. Guevara-Patiño, University of Chicago, Section of General Surgery, 5841 S. Maryland Avenue, MC 7114, Chicago, Illinois 60637, USA. Phone: (773) 702-5438. Fax: (773) 834-8140. E-mail: jguevara@surgery.bsd.uchicago.edu.

Mary Jo Turk's present address is: Norris Cotton Cancer Center, Dartmouth-Hitchcock Medical Center, Lebanon, New Hampshire, USA.

1. Overwijk, W.W., and Restifo, N.P. 2000. Autoimmunity and the immunotherapy of cancer: targeting the "self" to destroy the "other". *Crit. Rev. Immunol.* **20**:433–450.
2. Houghton, A.N., and Guevara-Patino, J.A. 2004. Immune recognition of self in immunity against cancer. *J. Clin. Invest.* **114**:468–471. doi:10.1172/JCI200422685.
3. Nikolic-Zugic, J., and Bevan, M.J. 1990. Role of self-peptides in positively selecting the T-cell repertoire. *Nature.* **344**:65–67.
4. Tanchot, C., Lemonnier, F.A., Perarnau, B., Freitas, A.A., and Rocha, B. 1997. Differential requirements for survival and proliferation of CD8 naive or memory T cells. *Science.* **276**:2057–2062.
5. Ernst, B., Lee, D.S., Chang, J.M., Sprent, J., and Surh, C.D. 1999. The peptide ligands mediating positive selection in the thymus control T cell survival and homeostatic proliferation in the periphery. *Immunity.* **11**:173–181.
6. Kieper, W.C., Burghardt, J.T., and Surh, C.D. 2004. A role for TCR affinity in regulating naive T cell homeostasis. *J. Immunol.* **172**:40–44.
7. Stefanova, I., Horejsi, V., Ansotegui, I.J., Knapp, W., and Stockinger, H. 1991. GPI-anchored cell-surface molecules complexed to protein tyrosine kinases. *Science.* **254**:1016–1019.
8. Townsend, S.E., and Allison, J.P. 1993. Tumor rejection after direct costimulation of CD8+ T cells by B7-transfected melanoma cells. *Science.* **259**:368–370.
9. Kaplan, M.H., and Craig, J.M. 1963. Immunologic studies of heart tissue. VI. Cardiac lesions in rabbits associated with autoantibodies to heart induced by immunization with heterologous heart. *J. Immunol.* **90**:725–733.
10. Tanaka, N., Nishimura, T., Tada, T., and Okabayashi, A. 1964. Autoimmune phenomenon occurred in the course of prolonged stimulation of heterologous protein. *Jpn. J. Exp. Med.* **34**:53–57.
11. Weigle, W.O. 1965. The induction of autoimmunity in rabbits following injection of heterologous or altered homologous thyroglobulin. *J. Exp. Med.* **121**:289–308.
12. Naftzger, C., et al. 1996. Immune response to a differentiation antigen induced by altered antigen: a study of tumor rejection and autoimmunity. *Proc. Natl. Acad. Sci. U. S. A.* **93**:14809–14814.
13. Overwijk, W.W., et al. 1998. gp100/pmel 17 is a murine tumor rejection antigen: induction of "self"-reactive, tumoricidal T cells using high-affinity, altered peptide ligand. *J. Exp. Med.* **188**:277–286.
14. Weber, L.W., et al. 1998. Tumor immunity and autoimmunity induced by immunization with homologous DNA. *J. Clin. Invest.* **102**:1258–1264.
15. Bowne, W.B., et al. 1999. Coupling and uncoupling of tumor immunity and autoimmunity. *J. Exp. Med.* **190**:1717–1722.
16. Hawkins, W.G., et al. 2000. Immunization with DNA coding for gp100 results in CD4 T-cell independent antitumor immunity. *Surgery.* **128**:273–280.
17. Hawkins, W.G., et al. 2002. Xenogeneic DNA immunization in melanoma models for minimal residual disease. *J. Surg. Res.* **102**:137–143.
18. Dyall, R., et al. 1998. Heteroclitic immunization induces tumor immunity. *J. Exp. Med.* **188**:1553–1561.
19. Gold, J.S., et al. 2003. A single heteroclitic epitope determines cancer immunity after xenogeneic DNA immunization against a tumor differentiation antigen. *J. Immunol.* **170**:5188–5194.
20. Rudolph, M.G., and Wilson, I.A. 2002. The specificity of TCR/pMHC interaction. *Curr. Opin. Immunol.* **14**:52–65.
21. Tai, T., Eisinger, M., Ogata, S.-I., and Lloyd, K.O. 1983. Glycoproteins as differentiation markers in human malignant melanoma and melanocytes. *Cancer Res.* **43**:2773–2777.
22. Vijayasaradhi, S., Bouchard, B., and Houghton, A.N. 1990. The melanoma antigen gp75 is the human homologue of the mouse b (brown) locus gene product. *J. Exp. Med.* **171**:1375–1380.
23. Overwijk, W.W., et al. 1999. Vaccination with a recombinant vaccinia virus encoding a "self" antigen induces autoimmune vitiligo and tumor cell destruction in mice: requirement for CD4(+) T lymphocytes. *Proc. Natl. Acad. Sci. U. S. A.* **96**:2982–2987.
24. Wolchok, J.D., et al. 2001. Alternative roles for interferon-gamma in the immune response to DNA vaccines encoding related melanosomal antigens. *Cancer Immun.* **1**:9.
25. Overwijk, W.W., et al. 2003. Tumor regression and autoimmunity after reversal of a functionally tolerant state of self-reactive CD8+ T cells. *J. Exp. Med.* **198**:569–580.
26. Barouch, D.H., et al. 2001. Elicitation of high-frequency cytotoxic T-lymphocyte responses against both dominant and subdominant simian-human immunodeficiency virus epitopes by DNA vaccination of rhesus monkeys. *J. Virol.* **75**:2462–2467.
27. Subbramanian, R.A., et al. 2003. Magnitude and diversity of cytotoxic-T-lymphocyte responses elicited by multiepitope DNA vaccination in rhesus monkeys. *J. Virol.* **77**:10113–10118.
28. Parker, K.C., Shields, M., DiBrino, M., Brooks, A., and Coligan, J.E. 1995. Peptide binding to MHC class I molecules: implications for antigenic peptide prediction. *Immunol. Res.* **14**:34–57.
29. Huard, R., Dyall, R., and Nikolic-Zugic, J. 1997. The critical role of a solvent-exposed residue of an MHC class I-restricted peptide in MHC-peptide binding. *Int. Immunol.* **9**:1701–1707.
30. Dyall, R., Fremont, D.H., Jameson, S.C., and Nikolic-Zugic, J. 1996. T cell receptor (TCR) recognition of MHC class I variants: intermolecular second-site reversion provides evidence for peptide/MHC conformational variation. *J. Exp. Med.* **184**:253–258.
31. Vijayasaradhi, S., Xu, Y., Bouchard, B., and Houghton, A.N. 1995. Intracellular sorting and targeting of melanosomal membrane proteins: identification of signals for sorting of the human brown locus protein, gp75. *J. Cell Biol.* **130**:807–820.
32. Roux, L., and Lloyd, K.O. 1986. Glycosylation characteristics of pigmentation-associated antigen (GP75): an intracellular glycoprotein of human melanocytes and malignant melanomas. *Arch. Biochem. Biophys.* **251**:87–96.
33. Vijayasaradhi, S., Doskoch, P.M., and Houghton, A.N. 1991. Biosynthesis and intracellular movement of the melanosomal membrane glycoprotein gp75, the human b (brown) locus product. *Exp. Cell Res.* **196**:233–240.
34. Xu, Y., et al. 2001. Diverse roles of conserved asparagine-linked glycan sites on tyrosinase family glycoproteins. *Exp. Cell Res.* **267**:115–125.
35. Xu, Y., Setaluri, V., Takechi, Y., and Houghton, A.N. 1997. Sorting and secretion of a melanosome membrane protein, gp75/TRP1. *J. Invest. Dermatol.* **109**:788–795.
36. Ostankovitch, M., Robila, V., and Engelhard, V.H. 2005. Regulated folding of tyrosinase in the endoplasmic reticulum demonstrates that misfolded full-length proteins are efficient substrates for class I processing and presentation. *J. Immunol.* **174**:2544–2551.
37. Dorner, A.J., et al. 1990. The stress response in Chinese hamster ovary cells. Regulation of ERp72 and protein disulfide isomerase expression and secretion. *J. Biol. Chem.* **265**:22029–22034.
38. Travers, K.J., et al. 2000. Functional and genomic analyses reveal an essential coordination between the unfolded protein response and ER-associated degradation. *Cell.* **101**:249–258.
39. Xu, Y., Vijayasaradhi, S., and Houghton, A.N. 1998. The cytoplasmic tail of the mouse brown locus product determines intracellular stability and export from the endoplasmic reticulum. *J. Invest. Dermatol.* **110**:324–331.
40. Ulmer, J.B., Donnelly, J.J., and Liu, M.A. 1994. Presentation of an exogenous antigen by major histocompatibility complex class I molecules. *Eur. J. Immunol.* **24**:1590–1596.
41. Lippolis, J.D., et al. 2000. Pseudomonas exotoxin-mediated delivery of exogenous antigens to MHC class I and class II processing pathways. *Cell Immunol.* **203**:75–83.
42. Hung, C.F., et al. 2001. Cancer immunotherapy using a DNA vaccine encoding the translocation domain of a bacterial toxin linked to a tumor antigen. *Cancer Res.* **61**:3698–3703.
43. Theobald, M., et al. 1997. Tolerance to p53 by A2.1-restricted cytotoxic T lymphocytes. *J. Exp. Med.* **185**:833–841.
44. Britten, C.M., et al. 2002. The use of HLA-A*0201-transfected K562 as standard antigen-presenting cells for CD8(+) T lymphocytes in IFN-gamma ELISPOT assays. *J. Immunol. Methods.* **259**:95–110.
45. LaFace, D.M., et al. 1995. Human CD8 transgene regulation of HLA recognition by murine T cells. *J. Exp. Med.* **182**:1315–1325.
46. Sherman, L.A., Hesse, S.V., Irwin, M.J., La Face, D., and Peterson, P. 1992. Selecting T cell receptors with high affinity for self-MHC by decreasing the contribution of CD8. *Science.* **258**:815–818.
47. Borbulevych, O.Y., Baxter, T.K., Yu, Z., Restifo, N.P., and Baker, B.M. 2005. Increased immunogenicity of an anchor-modified tumor-associated antigen is due to the enhanced stability of the peptide/MHC complex: implications for vaccine design. *J. Immunol.* **174**:4812–4820.
48. Chen, J.L., et al. 2005. Structural and kinetic basis for heightened immunogenicity of T cell vaccines. *J. Exp. Med.* **201**:1243–1255.
49. Messaoudi, I., Guevara Patino, J.A., Dyall, R., LeMaoult, J., and Nikolich-Zugich, J. 2002. Direct link between mhc polymorphism, T cell avidity, and diversity in immune defense. *Science.* **298**:1797–1800.
50. Dalod, M., et al. 1999. Broad, intense anti-human immunodeficiency virus (HIV) ex vivo CD8(+) responses in HIV type 1-infected patients: comparison with anti-Epstein-Barr virus responses and changes during antiretroviral therapy. *J. Virol.* **73**:7108–7116.
51. Pantaleo, G., et al. 1997. The qualitative nature of the primary immune response to HIV infection is a prognosticator of disease progression independent of the initial level of plasma viremia. *Proc. Natl. Acad. Sci. U. S. A.* **94**:254–258.
52. Day, C.L., et al. 2002. Broad specificity of virus-specific CD4+ T-helper-cell responses in resolved hepatitis C virus infection. *J. Virol.* **76**:12584–12595.
53. Kim, A.Y., et al. 2005. The magnitude and breadth of hepatitis C virus-specific CD8+ T cells depend on absolute CD4+ T-cell count in individuals coinfected with HIV-1. *Blood.* **105**:1170–1178.
54. Khong, H.T., and Restifo, N.P. 2002. Natural selection of tumor variants in the generation of "tumor escape" phenotypes. *Nat. Immunol.* **3**:999–1005.
55. Vitiello, A., Marchesini, D., Furze, J., Sherman, L.A., and Chesnut, R.W. 1991. Analysis of the HLA-restricted influenza-specific cytotoxic T lymphocyte response in transgenic mice carrying a chimeric human-mouse class I major histocompatibility complex. *J. Exp. Med.* **173**:1007–1015.
56. Scheibenbogen, C., et al. 1997. A sensitive ELISPOT assay for detection of CD8+ T lymphocytes specific for HLA class I-binding peptide epitopes derived from influenza proteins in the blood of healthy donors and melanoma patients. *Clin. Cancer Res.* **3**:221–226.